Synergic green technologies for treatment of hexavalent chromium polluted waters
Project PNII-RU-TE-2014-4-0508
No. 129/1/10/2015

Scientific report

Phase 3: 01.01.2017 – 30.09.2017

Objective 1. Ensuring the necessary conditions for the research activities
Activities: The needed existent materials have been identified and prepared. Other necessary but not existent materials have been purchased (flocculator, micropipette, micropipette tips, electrodes, water distiller, hotplate stirrer, reagents, tubes for peristaltic pump). The analytical methods have been selected and prepared in order to support the research activities.

Objective 2. Investigation of the effect of manganese oxide coated sand co-presence on Cr(VI) removal with Fe^0
Activities: Batch and column treatability experiments for Cr(VI) removal with Fe^0 in the co-presence of manganese oxide coated sand

2.1. Materials and methods

2.1.1. Preparation of manganese oxide coated sand

For this phase we used sand obtained from a local source, which was sieved to obtain the grain size 0.5-1.25 mm; the sand was then washed with distilled water and dried. All other reagents employed in this study were of analytical grade.

2.1.1.1. Method 1

A $MnSO_4$ solution was added drop wise (30 minutes) to an alkaline $KMnO_4$ solution containing 100 g of sand, while keeping vigorously stirred (hotplate stirrer Witeg MSH-20D); the solution turned to dark, indicating the formation of MnO_2 according to the reaction:

$$2H_2O + 3Mn^{2+} + 2MnO_4^- \rightarrow 5MnO_2 + 4H^+ \quad (1)$$

The molar ratio $MnSO_4$: $KMnO_4$: NaOH was 3:2:4. After the complete addition of $MnSO_4$ solution, the mixture was maintained under stirring for 60 minutes, and then aged for 24 h. The coated sand was filtered, washed with distilled water, and dried in an oven at 100 °C for 24 h. Previous works have shown that the as obtained oxide is δ-MnO_2 (birnessite) (Chaudhry et al., 2016; Landrot et al., 2010; Ma et al., 2013)

2.1.1.2. Method 2

A 0.3 M $MnSO_4$ solution was added drop wise (30 minutes) to a an alkaline 5% H_2O_2 solution containing 100 g of sand, while keeping vigorously stirred (hotplate stirrer Witeg MSH-20D); the solution turned to dark, indicating the formation of MnO_2 according to the reaction:

$$Mn^{2+} + H_2O_2 + 2HO^- \rightarrow MnO_2 + 2H_2O \quad (2)$$

After the complete addition of $MnSO_4$ solution, the mixture was maintained under stirring for 60 minutes, and then aged for 24 h. The coated sand was filtered, washed with distilled water, and dried in an oven at 100 °C for 24 h (Tilak et al., 2013; Wekesa et al, 2011).

2.1.1.3. Method 3

A 37% HCl solution was added drop wise (60 minutes) to a a hot (90 ^oC) $KMnO_4$ 1 N solution containing 100 g of sand, while keeping vigorously stirred (hotplate stirrer Witeg MSH-20D); the solution turned to dark, indicating the formation of MnO_2 according to the reaction:

$$2KMnO_4 + 8HCl \rightarrow 2MnO_2 + 2KCl + 3Cl_2 + 4H_2O \quad (3)$$

After the complete addition of HCl, the mixture was maintained under stirring for 60 minutes, and then cooled to room temperature and aged for 24 h. The coated sand was filtered, washed with distilled water, and dried in an oven at 100 °C for 24 h. Previous works have shown that the as obtained oxide is δ-MnO_2 (vernadite or birnessite) (Taffarel and Rubio, 2010; Manning 2002)

2.1.2. Batch treatability experiments for the removal of Cr(VI) with Fe^0 in co-presence of manganese oxide coated sand

Commercially available Fe^0 from Merck (≥ 99%, 10 μm) was used in this assay as received, together with the manganese oxide coated sand (sand/MnO_2) synthesized via methods 1-3. Batch treatability experiments were carried out in 800 mL Berzelius flasks, by introducing 0.25 g Fe^0 and 15 g sand/MnO_2 into 500 mL Cr(VI) solution 2 mg/L with pH 2.5, at room temperature (22 ± 2 ^oC). The mixture was stirred (200 rpm) using an Ovan agitator (Fig.1) and, at timed intervals, samples were withdrawn, filtered and analyzed for Cr(VI). pH 2.5 was selected because strong acidic pH was previously reported as optimum value for Cr(VI) removal with Fe^0 in batch system (Gheju and Iovi 2006).

Fig.1. Experimental setup of the batch treatability experiments

2.1.3. Column treatability experiments for the removal of Cr(VI) with Fe^0 in co-presence of manganese oxide coated sand

Commercially available Fe^0 from Alfa Aesar (≥ 99%, 1-2 mm) was used in this assay as received, together with the manganese oxide coated sand (sand/MnO_2) prepared via methods 1-3. The laboratory apparatus used for the flow-through column experiments consisted in polyethylene columns (inner diameter: 2 cm; height: 11 cm), an Ismatec IP08 peristaltic pump and a tank with a capacity of 60 L (Fig. 2). The columns were packed with fillings having different compositions, as summarized in table 1. Below and above the filling was a layer of 5 cm^3 sand with d = 1.25-2 mm. Cr(VI) stock solution (10 g/L) was prepared by dissolving 28.29 g $K_2Cr_2O_7$ in 1000 mL of distilled deionized water.

Fig.2. Experimental setup of the column treatability experiments

Table 1. Experimental setup of the column experiments

Column	Column filling				Cr(VI) solution		
	Fe^0		Sand		Concentration (mg/L)	pH	Flow (mL/h)
	(% vol.)	(cm^3)	(% vol.)	(cm^3)			
1	100	20	0	0	5	6,9	30
2	60	30	40	20[a]	5	6,9	30
3	60	30	40	20 M1[a]	5	6,9	30
4	60	30	40	20 M2[c]	5	6,9	30
5	60	30	40	20 M3[d]	5	6,9	30

a – sand;
b – sand /MnO_2 prepared via method 1;
c – sand /MnO_2 prepared via method 2;
d – sand /MnO_2 prepared via method 3;

Working solution of the desired initial Cr(VI) concentration (5 mg/L) was then prepared by diluting the stock solution with tap water, in order to simulate a case of natural water pollution. This concentration was selected because it is within the range of relevant concentrations for Cr(VI) polluted groundwaters (Flury et al., 2009; Wilkin et al., 2005). The pH was adjusted to 6.9 by small addition of concentrated H_2SO_4. The Cr(VI) working solution was passed through the column, at room temperature (22±2 ^oC), from the bottom to the top, and effluent samples were withdrawn at regular time intervals for the analysis of Cr(VI) concentration and pH.

2.1.4. Analytical procedure

Chromium and iron dissolved species were determined by spectrophotometric methods, using a Specord 200 Plus spectrophotometer (Standard Methods, 1995). Cr(VI) concentration was determined by the 1,5-diphenylcarbazide method, at 540 nm. The calibration curve of Cr(VI) is depicted in Fig 3. The pH was measured in samples using an Inolab 7320 pH-meter calibrated with three standards. Scanning electron microscopy - energy dispersive angle X-ray spectrometry (SEM-EDX, FEI Inspect S/GENESIS XM 2i) and X-ray diffraction spectroscopy (XRD, Phillips FEI X'Pert PRO MPD) were employed to investigate the chemistry and morphology of the sand/MnO_2 samples prepared via methods 1-3

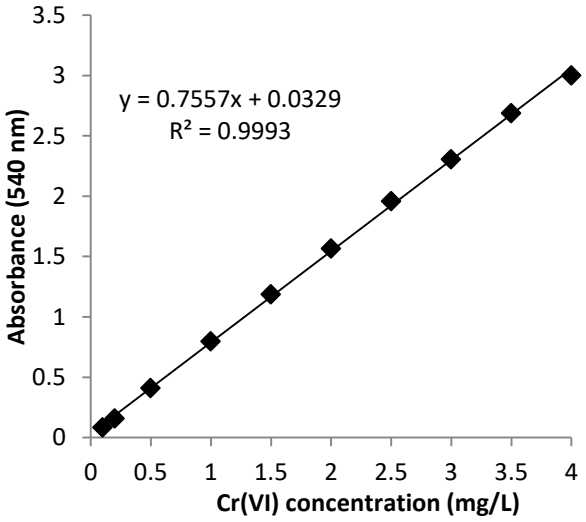

Fig.3. Cr(VI) calibration curve

2.2. Results and discussion

2.2.1. Characterization of the manganese oxide coated sand

The analysis of XRD (Fig. 4-7) patterns and of SEM images (Fig. 8-11) reveals no significant differences between the fresh sand and the manganese oxide coated sand prepared via methods 1-3. The fact that MnO_2 peaks were not observed in the XRD pattern of the manganese oxide coated sand samples is in accord with the reports made in previous studies, which suggested that this phenomenon can be ascribed to the low amounts of manganese oxide existent at the surface of the support, as well as to a highly dispersed distribution of these oxides at the surface of the support (Kapteijin et al., 1994; Maliyekkal et al., 2009). Nevertheless, the visual examination of the fresh sand and manganese oxide coated sand samples (Fig. 12) reveals they have different colors, confirming thus the existence of a manganese oxide layer at the surface of the sand samples prepared via methods 1-3. Figure 12 also indicates that efficiency of the process of coating sand with MnO_2 decreases in the order: Method 2 > Method 3 > Method 1. This is confirmed also by the EDX analysis (Fig 13-16) which shows that concentration of Mn at surface of sand was 8.7%, 1% and 0%, for the samples prepared via methods 2, 3, and 1, respectively.

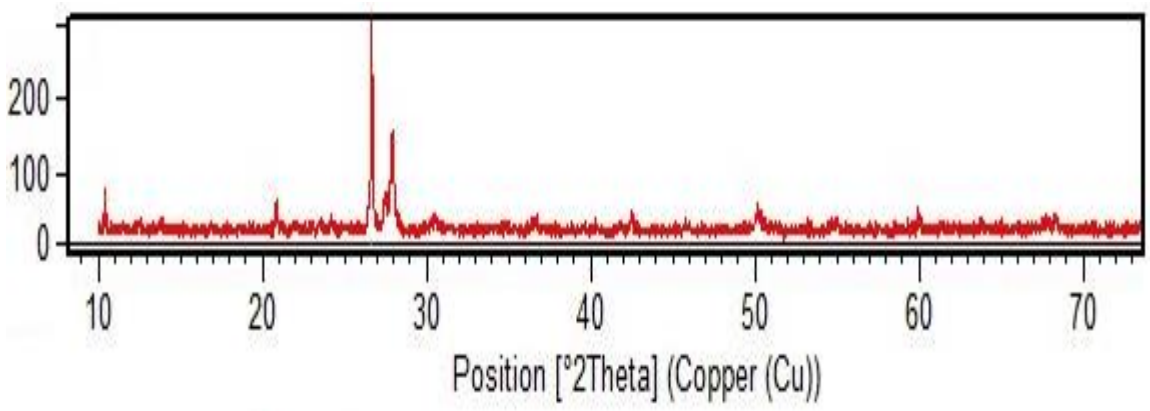

Fig.4. XRD pattern of sand

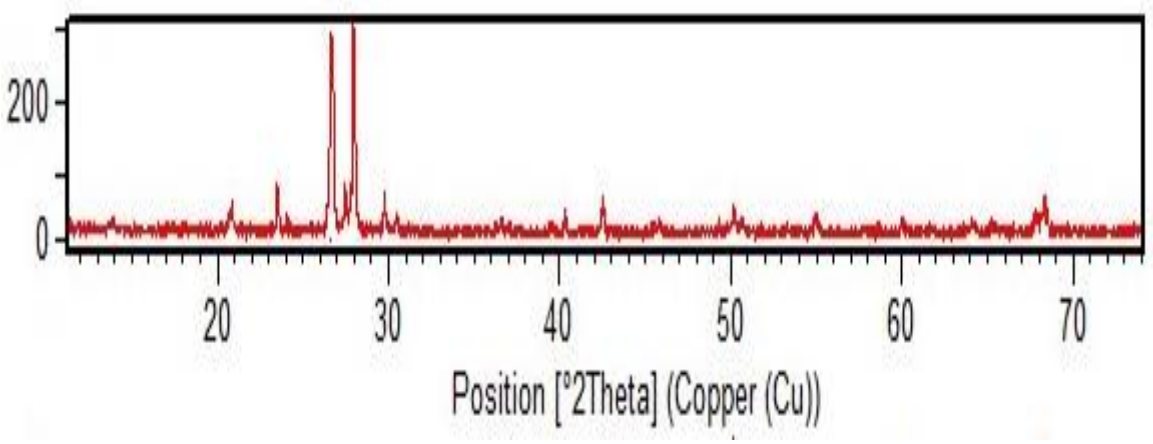

Fig.5. XRD pattern of sand/MnO_2 prepared via method 1

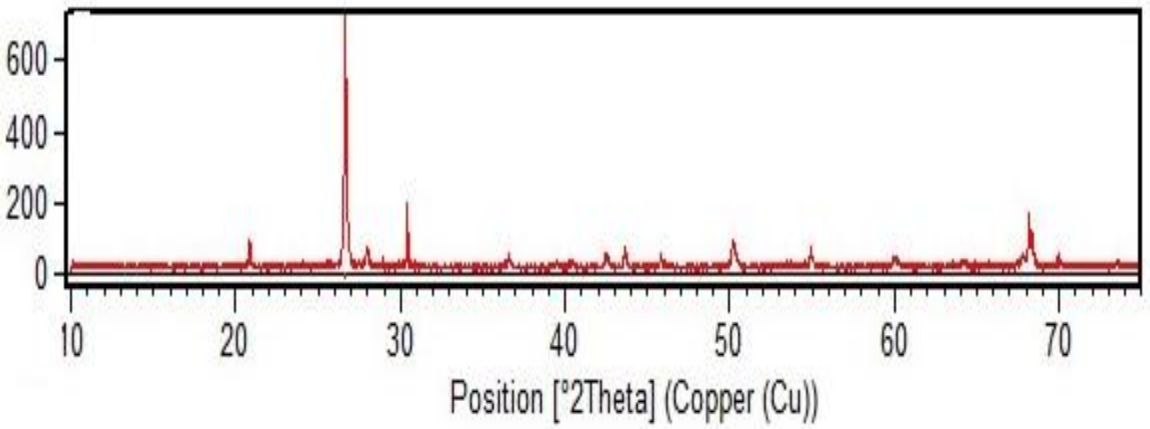

Fig.6. XRD pattern of sand/MnO_2 prepared via method 2

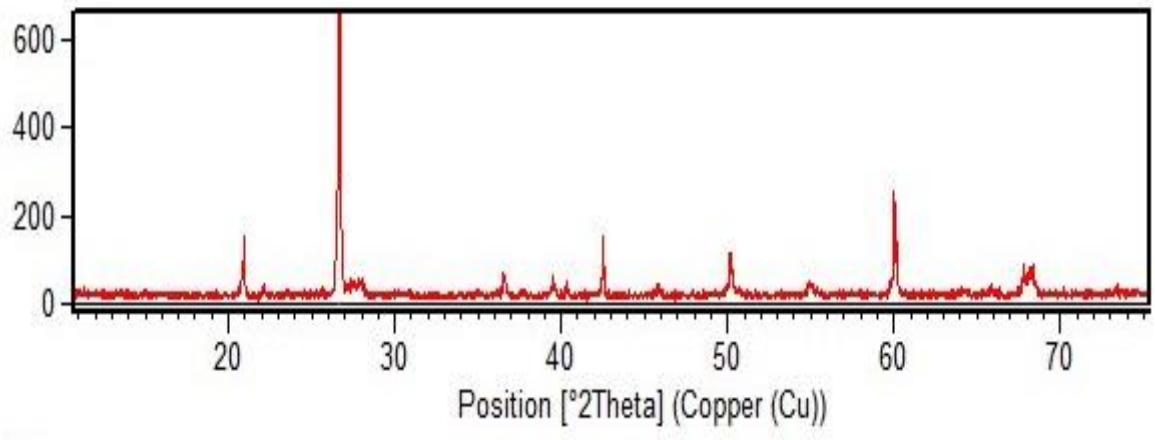

Fig.7. XRD pattern of sand/MnO_2 prepared via method 3

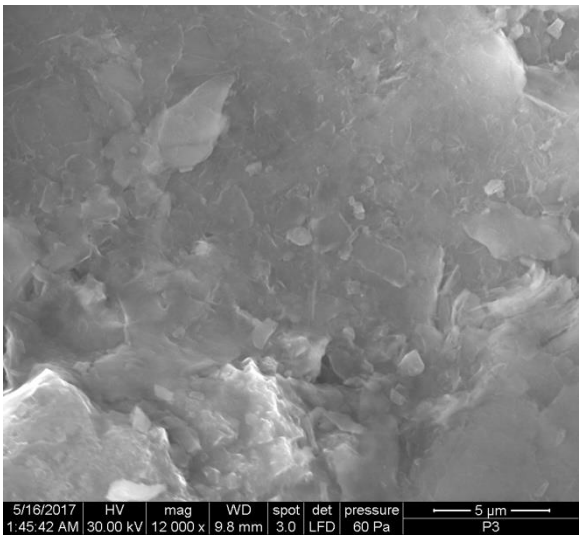

Fig.8. SEM micrograph of sand

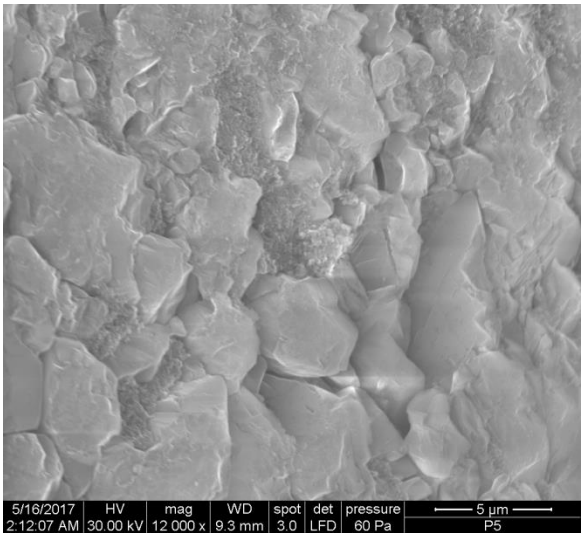

Fig.9. SEM micrograph of sand/MnO_2 prepared via method 1

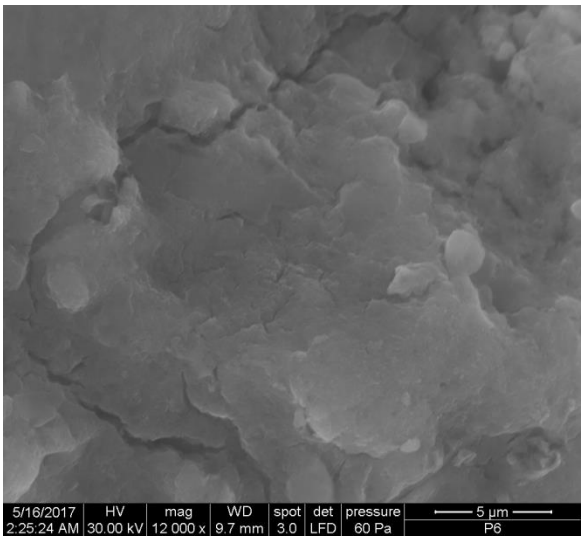

Fig.10. SEM micrograph of sand/MnO_2 prepared via method 2

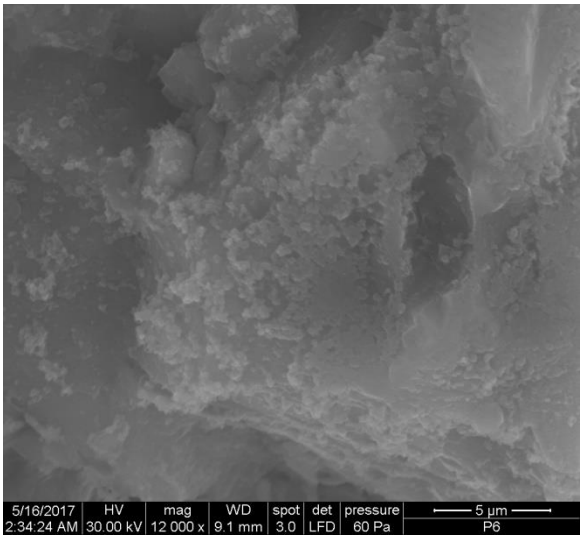

Fig.11. SEM micrograph of sand/MnO_2 prepared via method 3

Fig.12. Image of sand (0) and sand/MnO_2 samples prepared via methods 1-3

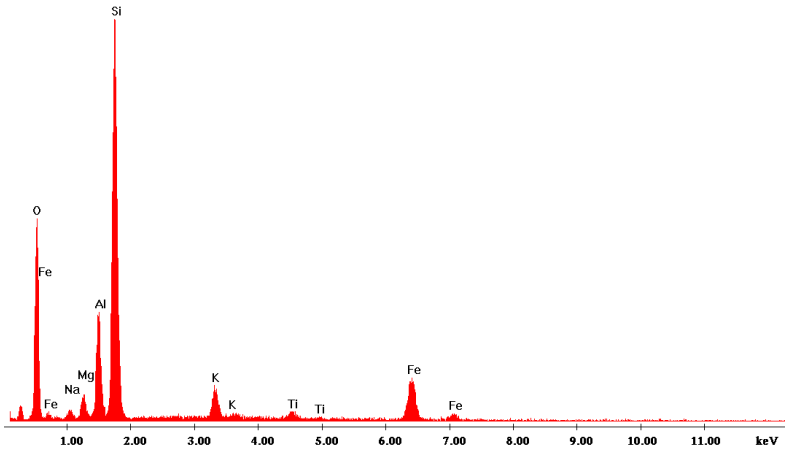

Fig.13. EDX pattern of sand

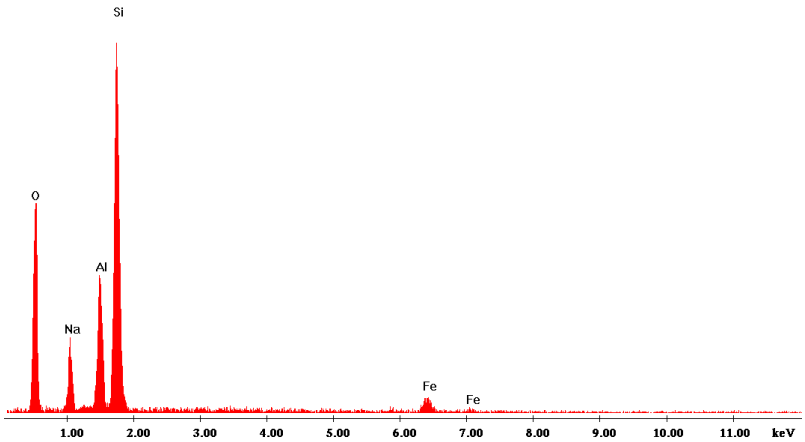

Fig.14. EDX pattern of sand/MnO_2 prepared via method 1

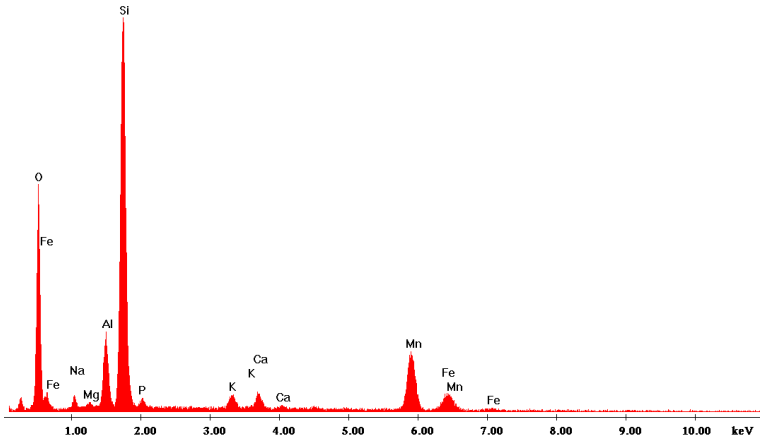

Fig.15. EDX pattern of sand/MnO_2 prepared via method 2

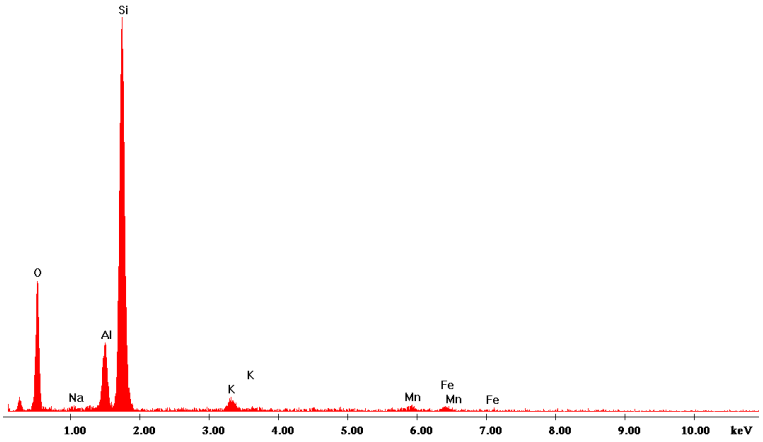

Fig.16. EDX pattern of sand/MnO_2 prepared via method 3

2.2.2. Batch experiments

The results of batch treatability experiments are shown in Fig. 17. From this figure it can be seen that there are no significant differences between experiments carried out with Fe^0 + sand and those with Fe^0 + sand/MnO_2. In the same time, it was noticed that removal of Cr(VI) with Fe^0 was favored in the presence of sand, regardless of its nature (untreated sand or sand/MnO_2). This is an accord with results of experiments conducted in phase 2 of this project (2016), when it was noticed an improvement of the efficiency of Cr(VI) removal with Fe^0 in co-presence of sand.

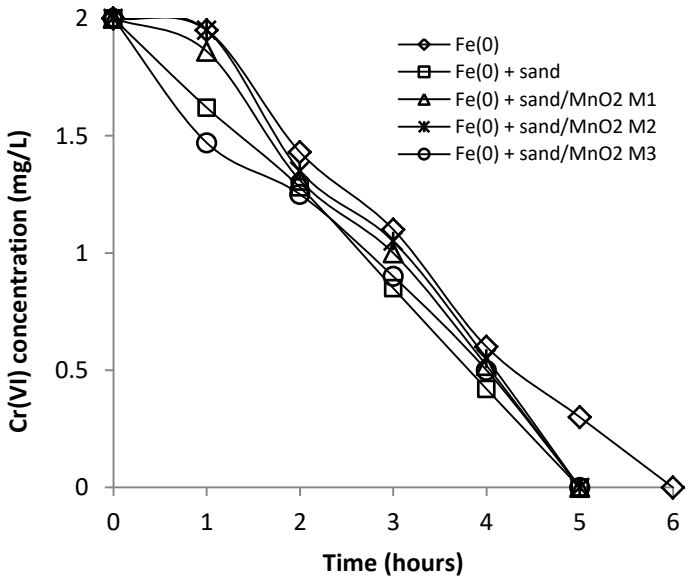

Fig. 17. Cr(VI) vs. time for removal experiments with Fe^0 + sand.

2.2.3. Column experiments

Fig.18 depicts the evolution of Cr(VI) concentration in the effluent of columns with various filling composition. From this figure it can be seen that better Cr(VI) removal efficacies were achieved for the column packed with Fe^0 + sand mixture, than when filling of columns was composed of Fe^0 + sand/MnO_2, regardless of the method used for the preparation of sand/MnO_2. Column breakthrough occurred after 5 days in all columns containing Fe^0 + sand/MnO_2 filling, while in column with Fe^0 + sand filling the breakthrough was noticed only in the 7^{th} day. This observation is in agreement with the results of the experiments carried out in phase 2 of this project (2016), when it was reported that removal of Cr(VI) with Fe^0 was detrimentally affected by the co-presence of MnO_2. However, it should be mentioned that for all columns with Fe^0 + sand, regardless of the nature of sand (with or without coated MnO_2), better removal Cr(VI)efficiencies were obtained than for the column filled with bare Fe^0, for which the breakthrough was noticed in the 4^{th} day. This observation is also in agreement with the results of the experiments carried out in phase 2 of this project (2016), when it was noticed that removal of Cr(VI) with Fe^0 was enhanced in the co-presence of sand.

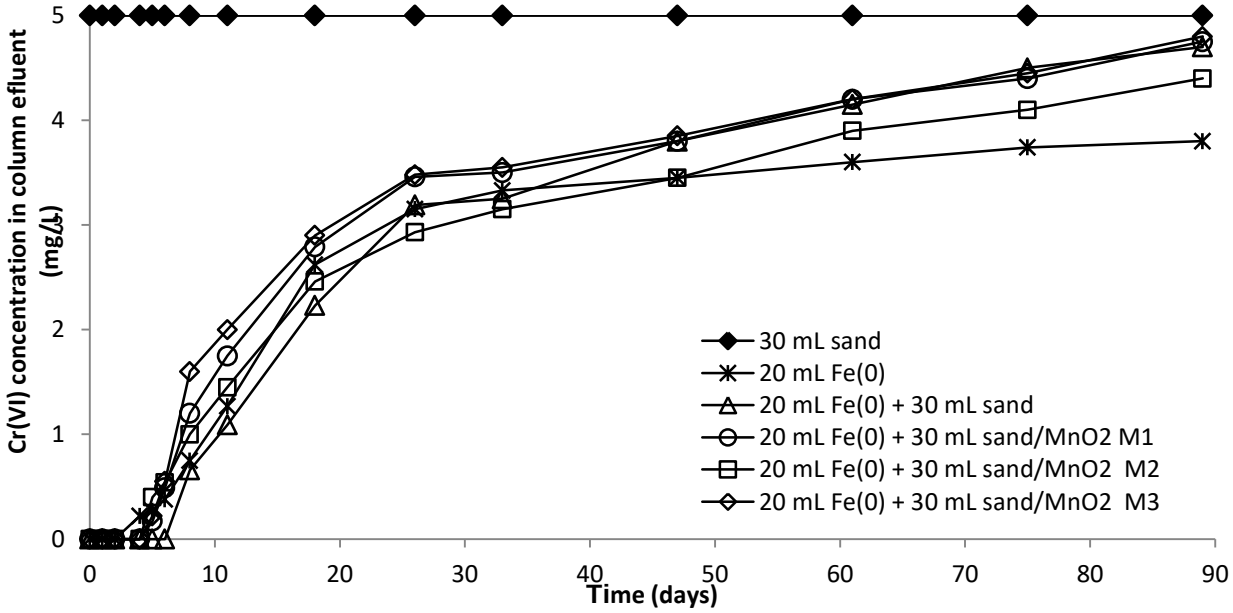

Fig. 18. Cr(VI) concentration in column effluent vs. time, for columns with various filling composition

Fig.19 shows that pH of the effluent increases significantly after the first days, while decreasing gradually thereafter until the end of experiment, when it reaches a steady-state. The initial increase of the pH is determined by the corrosion of Fe^0 in the co-presence of oxidants like Cr(VI), O_2 or H_2O, which takes place with consumption of protons and generation of hydroxyl ions, according to: (Gheju, 2011):

$$3Fe^0 + Cr_2O_7^{2-} + 14H^+ \rightarrow 3Fe^{2+} + 2Cr^{3+} + 7H_2O \quad (4)$$

$$6Fe^{2+} + Cr_2O_7^{2-} + 14H^+ \rightarrow 6Fe^{3+} + 2Cr^{3+} + 7H_2O \quad (5)$$

$$2Fe^0 + O_2 + 2H_2O \rightarrow 2Fe^{2+} + 4HO^- \quad (6)$$

$$Fe^0 + 2H_2O \rightarrow Fe^{2+} + H_2 + 2HO^- \quad (7)$$

The subsequent decrease in pH is due to reduction in intensity of the Cr(VI) reduction and Fe^0 corrosion, as a result of precipitation on the surface of Fe^0 of the above-mentioned solid mineral phases. Fig. 19 also indicates that highest initial pH increase was noticed for the column packed with Fe^0 + sand; this suggests the existence of more intense Fe^0 corrosion processes, and therefore, the generation of higher amounts of secondary reducing species which can convert Cr(VI) to Cr(III). This is in accord with the better removal efficacies achieved when filling of columns was composed of Fe^0 + sand. Apart from the first 10 days of the experiment, there are no important differences between the evolution of pH in effluent of columns filled with Fe^0 + sand/MnO_2 mixture and of the column with Fe^0 + sand filling.

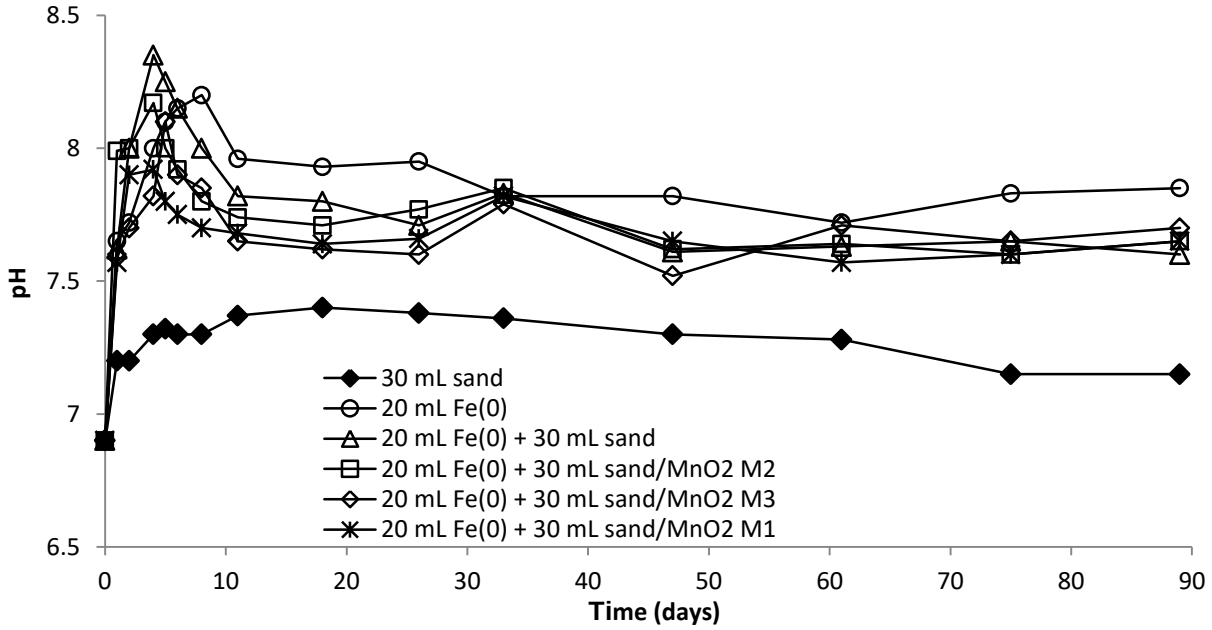

Fig. 19. pH in column effluent vs. time, for columns with various filling composition.

2.3. Conclusions

Batch and column treatability experiments carried out in this study indicated that co-presence of manganese oxide coated sand has a positive effect on the removal of Cr(VI) with Fe^0. Nevertheless, column experiments also revealed that better Cr(VI) removal efficacies were achieved for the column packed with Fe^0 + sand, than when filling of columns was composed of Fe^0 + sand/MnO_2, regardless of the method used for the preparation of sand/MnO_2. Therefore, it can be presumed that the positive effect was the result of sand co-presence, and not the result of coating sand with MnO_2. This can be ascribed to the fact that co-presence of sand may sustain the Fe^0-systems efficiency by improving the contact between water and Fe^0 and by delaying the reduction of column permeability due to corrosion products and precipitates that progressively fill the pore space.

Objective 3. Investigation of the alternative to immobilize exhausted reactive mixtures in vitreous matrices.

Activities: Experiments for the synthesis and characterization of glasses from exhausted reactive mixtures

3.1 Immobilization of the retained chromium from exhausted reactive mixtures containing Fe(0) in glass matrices

The immobilization of the exhausted reactive mixtures was realized by vitrification together with two types of common glass wastes: window panes and cathode ray tubes (CRT).

3.1.1 Experimental procedure

The compositions of the precursor glass wastes, determined by X ray fluorescence using a Niton XL 3 analyzer, are presented in table 2

Table 2. Oxidic composition of the precursor glass wastes [wt. %]

Oxide	Window pane	CRT
SiO_2	71,86	60,92
Na_2O	13,13	8,96
K_2O	0,02	7,44
CaO	9,23	0,67
MgO	5,64	0,14
BaO	-	10,80
PbO	-	8,85
Al_2O_3	0,08	2,07
Fe_2O_3	0,04	0,15

The two glass wastes were powdered by wet grinding using a Pulverisette laboratory mill than dried and sieved so that the granulometric fraction under 100 μm was kept in order to be used as glass precursor (Lazău and Vancea 2013).

The composition of the exhausted reactive mixture and the corresponding retained chromium from each column is presented in the table 3.

Table 3. The composition of the exhausted reactive mixture and the corresponding retained chromium [g].

Column	Fe^0 fraction 1-2 mm	Sand fraction 0.5-1.25 mm	Sand fraction 1.25-2 mm	Retained chromium [mg]
0	80	43.8	7.4	112
1	80	43.8	7.4	104
2	80	43.8	7.4	124
3	80	43.8	7.4	101

Considering that the 4 exhausted reactive mixtures have the same composition and granulometry, differing by the way the manganese oxide was coated, the sample used for the following investigations was the one from the column 2, having the highest amount of retained chromium (124 mg).

The exhausted reactive mixtures were dried at 105°C for 24 hours and then mixed together with the glass waste precursors.

The melting process was conducted at 1000°C for 180 minutes using a Nabertherm HTC08/16 electric furnace. The vitrification of the two types of wastes (glass and the reactive mixture containing chromium) in this economically advantageous conditions led to very viscous melts that were difficult to process. Therefore it was considered necessary to use borax as a flux in order to improve the fluidity of the melted glasses.

Four weight ratios exhausted reactive mixture-glass waste-borax were tested: 2:1:1, 1:1:1, 1:2:1 and 1:1:2, the obtained glasses are presented in figure 20

Fig.20. Glasses obtained using three different weight ratios exhausted reactive mixture-glass waste-borax.

The sample corresponding to the exhausted reactive mixture-glass waste-borax 2:1:1 generates a partial vitrified mass, removed from future investigations. The increase of the flux amount have a positive effect upon the glass fluidity due to the fondant effect of the two oxides brought by borax: Na_2O and B_2O_3. The negative effect of the flux is the fragilization of the glass matrix due to the destructive effect of the alkaline oxide upon the vitreous structure. The composition of the glass samples is presented in table 4.

Table 4. Composition of the studied glasses

Sample	Exhausted reactive mixture	Glass waste		Borax
		Geam	CRT	
1-G	1	1	-	1
2-G	1	2	-	1
3-G	1	1	-	2
1-C	1	-	1	1
2-C	1	-	2	1
3-C	1	-	1	2

3.1.2 Properties of the obtained glasses

Considering the objective of this study – to immobilize the exhausted reactive mixtures containing chromium in vitreous matrices – the investigated properties for the obtained glasses were the phase composition and the chemical resistance towards chemical aggression.

3.1.2.1 Phase composition of the studied glasses

The phase composition of the studied glass samples was determined using a Rigaku Ultima 4 diffractometer.

The diffraction spectra corresponding to the samples 1-G and 1-C, containing the highest amount of coarse sand, susceptible to remain unitegrated in the vitreous matrix at the considered melting temperature, and therefore generating specific SiO_2 peaks on the RX diffractogram, are presented in figure 21.

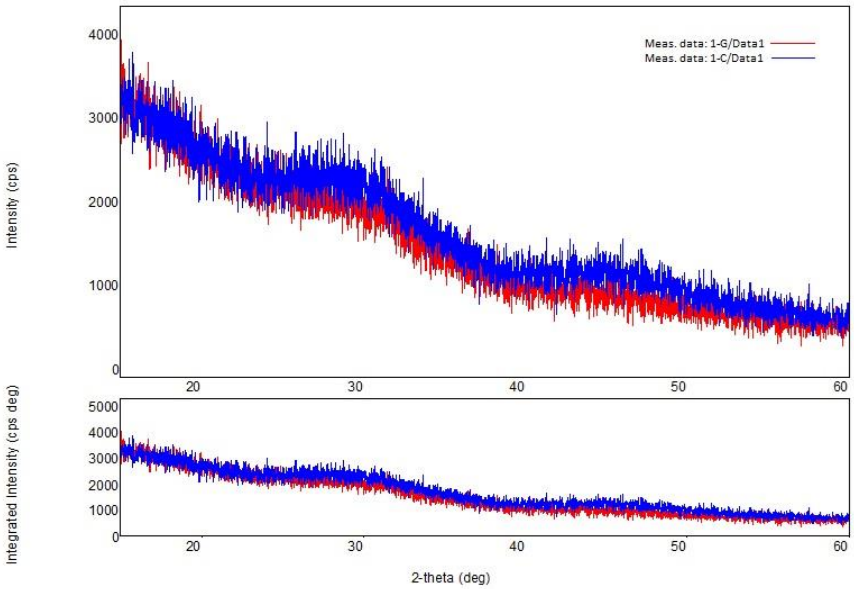

Fig.21. Diffraction spectra of the samples 1-G and 1-C

The diffuse pattern of both spectra confirm the amorphous character of the samples, confirming the purposed melting conditions.

3.1.2.2 Glasses hydrolytic stability

The hydrolytic stability of the glass ceramic samples was determined according to ISO 719-1985 (ISO 719-1985), using 2 grams of product, having particles size less than 500 μm, kept for 60 min in 50 mL de-ionized water at 98°C. A volume of 25 mL of the obtained solution was titrated against 0.01 mol/l HCl solution. The volume of HCl needed for neutralization is recorded in order to express the equivalent R_2O extracted and the corresponding stability class. The obtained results are presented in table 5 and illustrated in figure 22.

Table 5. Extracted R_2O and hydrolytic stability classes for the studied glasses

Sample	**Alkali oxide leached [μg/g glass]**	**Stability class**
1-G	16,4	HGB1
2-G	17,1	HGB1
3-G	18,6	HGB1
1-C	14,8	HGB1
2-C	16,2	HGB1

3-C	16,05	HGB1

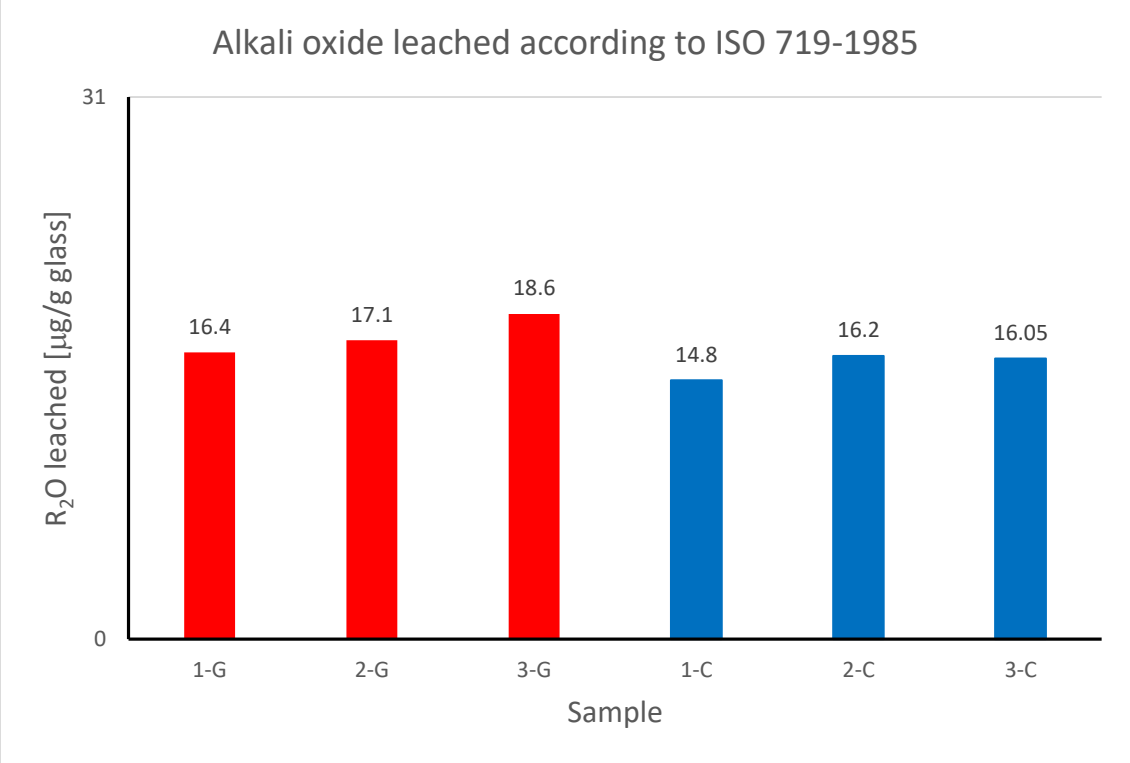

Fig.22. Evolution of alkali oxide losses in the investigated samples

All the studied glasses belongs to the most stable class of glasses HGB1. Increasing the borax amount in the samples 3-G and 3-C respectively leads to a rise of the losses of alkali oxide due to the supplementary amount of R_2O brought by the borax itself. The lowest losses were recorded for the samples 1-G and 1-C, having the least alkali oxide amount in their composition, as it is illustrated in the figure 23.

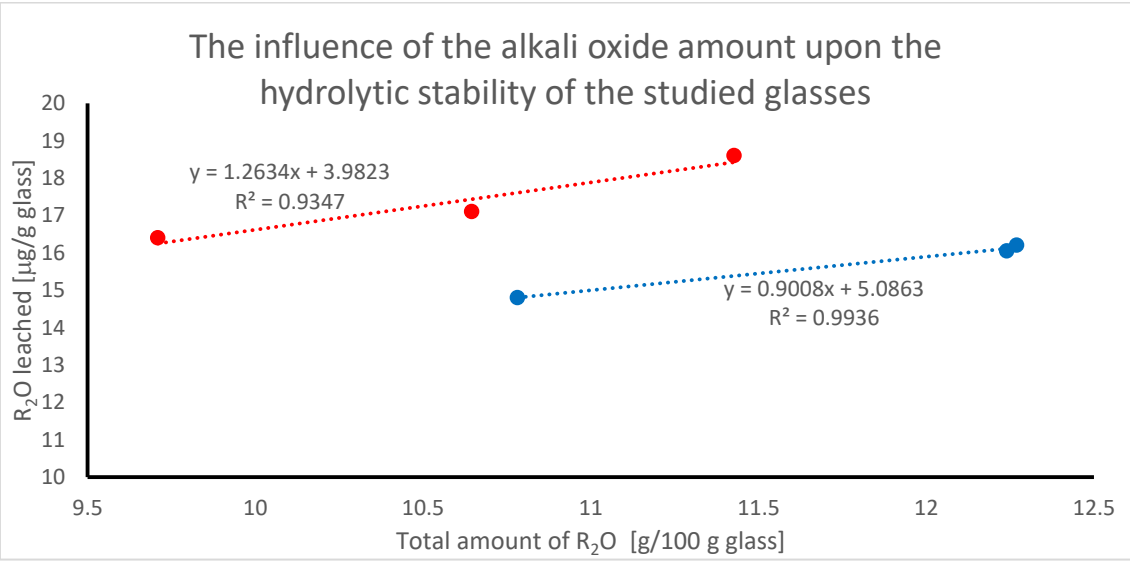

Fig. 23 The influence of the alkali oxide amount upon the glasses hydrolytic stability.

A quasiliniar dependence can be observed for both investigated glasses between the losses of R_2O, extracted from the glass in the mentioned conditions and the total amount of alkali oxide in the glass composition.

3.1.2.3. Chemical stability of the studied glasses

The chemical stability of the glasses was investigated by measuring the dissolution rate of the samples immersed in three extraction mediums having pH 5.5, 7.0 and 8.5 respectively for 28 days. The volume of the utilized solutions of 100 mL was maintained constant during the considered determination time at a constant temperature of 20 ± 2°C. After 28 days the samples were dried for 6 hours at 110°C until they reach constant mass. The dissolution rate of the glass samples is expressed as weight loss in time as it is presented in equation 8.

$$\mathrm{Dr} = \frac{\Delta \mathrm{m}}{t} = \frac{m_i - m_f}{t} \ [\mu g/h] \qquad (8)$$

where: m_i is the initial sample mass, m_f the final sample mass and t represents the considered experimental time of 28 days.

The calculated values for the dissolution rate of the investigated samples are presented in the table 6 and illustrated in the figure 24.

Table 6. Dissolution rates of the studied glasses [μg/h]

Sample	pH		
	pH=5.5	pH=7	pH=8.5
1-G	0,011	0,013	0,165
2-G	0,014	0,014	0,172
3-G	0,015	0,016	0,153
1-C	0,017	0,018	0,188
2-C	0,019	0,020	0,192
3-C	0,022	0,022	0,195

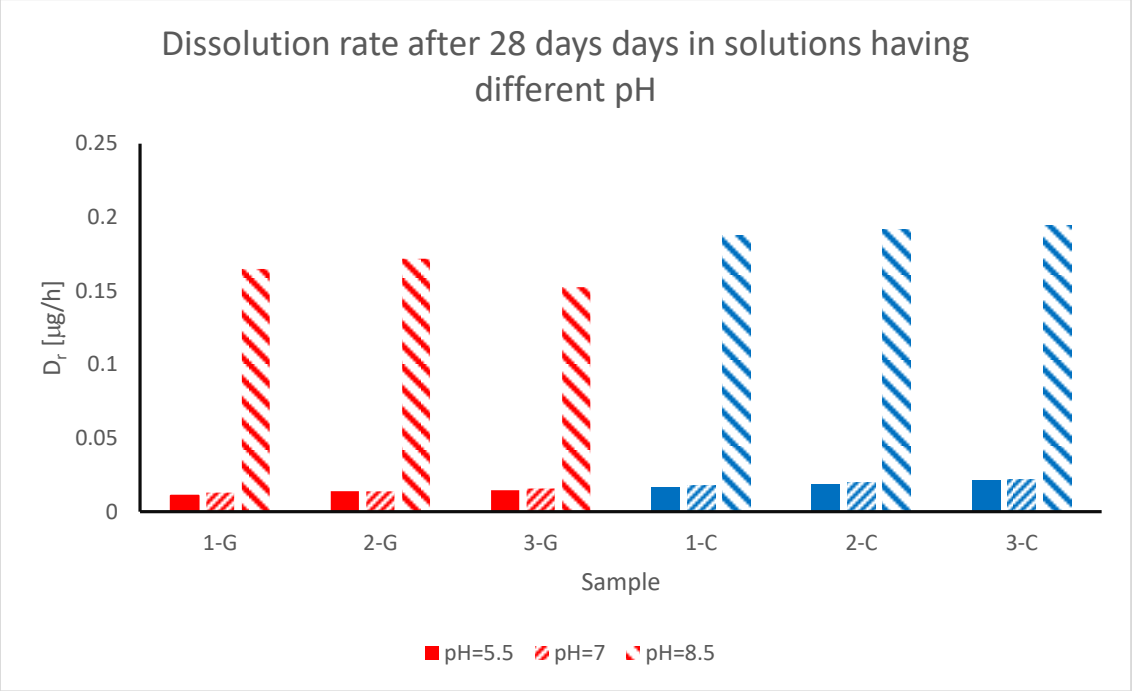

Fig.23. Dissolution rates of the studied glasses.

Two different behaviors can be observed, one for acidic and neutral mediums and another for alkaline medium. At pH = 5.5 and pH = 7.0 the glasses dissolution rates are very low, between 0,011-0,022 µg/h. This can be explain by the leaching of the alkali oxides from the glass surface in acidic and neutral mediums that lead to an enrichment in SiO_2 at the surface level. This oxide has an acidic character and therefore it is insoluble in the considered mediums. Consequently it creates a passivation effect that causes the lower dissolution rates values.

The alkaline environment leach SiO_2 and B_2O_3, both network former oxides, generating a continuous aggressive attack on the vitreous matrix. Without the passive layer the glasses are more sensitive to the alkaline medium and therefore the dissolution rate values are higher than in the previous case, between 0,153-0,195 µg/h.

3.1.2.4. Manganese, chromium and iron ions immobilization in glasses

The manganese, chromium and iron immobilization capacity of the studied glasses was investigated by measuring the chromium ions extraction using leaching tests performed according to the American Extraction Procedure Toxicity Test (US EPA625/6-89/022). Three extraction mediums having pH 5.5, 7.0 and 8.5 respectively were used, analysis being performed after 1, 14 and 28 days. The buffer solutions from 5.5, 7.0 and 8.5 pH were prepared by taking 2.5% v/v glacial acetic acid in water and by adding concentrated ammonia solution until the desired pH value was reached. The pH of the solution was measured using a digital pH meter (Type E-500). Two grams of each sample were taken and shaken with 250 mL of ammonia–acetate buffer solution for different time periods at a constant temperature of 20 ± 2°C. The chromium and iron concentration in the extraction mediums was measured using a Bruker Aurora M90 Inductively Coupled Plasma Mass Spectrometer.

None of the investigated samples show any loss of manganese ions, regardless the time and aggressive solution used.

The chromium ions leached from the studied glasses in the three chemical aggressive environments for the three considered periods of time are presented in the table 7 and illustrated in the figure 24.

Table 7. Chromium ions leached from the investigated glasses

Sample	Chromium ions leached [%]								
	7 days			14 days			28 days		
	pH=5.5	pH=7.0	pH=8.5	pH=5.5	pH=7.0	pH=8.5	pH=5.5	pH=7.0	pH=8.5
1-G	0	0	0	0,0041	0,0048	0,0112	0,0042	0,0042	0,0126
2-G	0	0	0	0,0033	0,0031	0,0109	0,0034	0,0033	0,0119
3-G	0	0	0	0,0047	0,0044	0,0104	0,0048	0,0045	0,0112
1-C	0	0	0	0,0038	0,0046	0,0085	0,0040	0,0040	0,0122
2-C	0	0	0	0,0040	0,0040	0,0088	0,0044	0,0043	0,0116
3-C	0	0	0	0,0044	0,0044	0,0091	0,0045	0,0044	0,0118

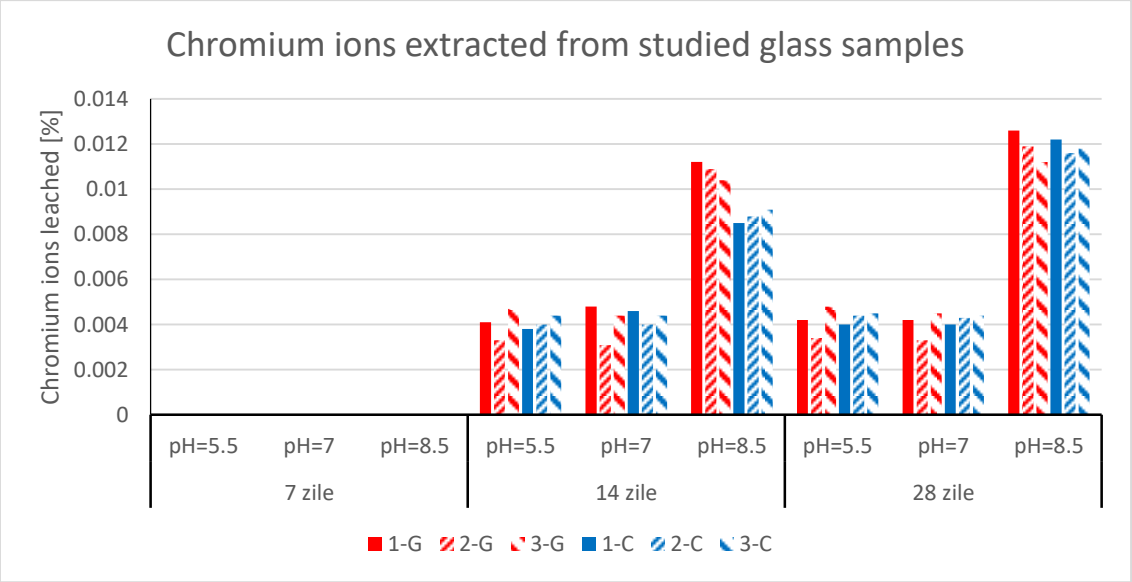

Fig.24. Chromium ions losses from the glasses containing exhausted reactive mixtures.

The amount of chromium ions leached from all the investigated glasses regardless the environment's pH and the considered time is very low, between 0-0,0121 % of the total chromium brought by the exhausted reactive mixtures.

The vitrification of the exhausted reactive mixtures leads to glass with no discernable losses of chromium after 7 days, regardless of the environment's pH. The chromium losses after 14 and 28 days respectively in acidic and neutral attack solutions are comparable while the alkaline attack leads to a higher chromium dissolution that rise as the attack period increase due to the lower resistance of the vitreous matrix upon the alkaline aggression.

The samples 1-G and 1-C, containing higher amounts of exhausted reactive mixtures have larger quantities of chromium leached since the mixture is the ion bearing vector.

The CRT glass generates at the synthesizing temperature more fluid melts comparing to window pane glass and therefore increase the chromium immobilization.

All the obtained glasses show higher chromium losses in alkaline environment compared to acid and neutral environments, due to the passivation effect discussed in chapter 3.1.2.3.

The iron ions losses for all the investigated samples are presented in the table 8 and illustrated in the figure 25.

Table 8. Iron ions leached from the investigated glasses

Sample	Iron ions leached [%]								
	7 days			14 days			28 days		
	pH=5.5	pH=7	pH=8.5	pH=5.5	pH=7	pH=8.5	pH=5.5	pH=7	pH=8.5
1-G	0	0	0	0	0	0,0017	0	0	0,0026
2-G	0	0	0	0	0	0	0	0	0,0023
3-G	0	0	0	0	0	0	0	0	0,0023
1-C	0	0	0	0	0	0,0014	0	0	0,0024
2-C	0	0	0	0	0	0,0011	0	0	0,0018
3-C	0	0	0	0	0	0	0	0	0,0015

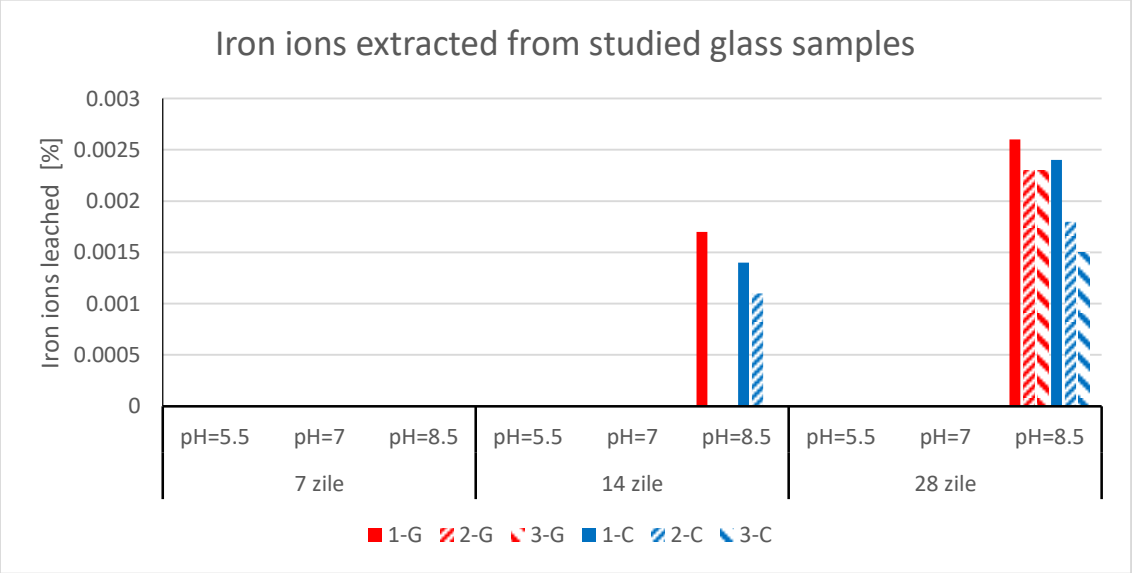

Fig.25. Iron ions losses from the studied glasses

The amount of iron ions leached from all the investigated glasses regardless the environment's pH and the considered time is very low, between 0-0,0026 % of the total iron brought by the exhausted reactive mixtures.

For all the samples no discernable iron losses have been recorded in acidic and neutral environments for the three considered periods of time.

Similarly to the previous discussion regarding the chromium losses, all glasses are more sensitive to the alkaline environment as it was explained before the effect is more present after 14 and especially after 28 days.

For all the glasses from this sets, increasing the amount of iron in the samples 1-G and 1-C leads to a lesser encapsulation of the iron ions in the glass network and consequently generates a lower immobilization.

3.1.3 Conclusions

- The focus of this research is to immobilize the chromium, manganese and iron ions retained on exhausted reactive mixtures by vitrification together with two common glass wastes: window panes and cathode ray tubes.
- Multiple ratios exhausted reactive mixture-glass wastes-borax were tested in order to establish the optimal synthesis conditions in order to obtain glasses comparable with the industrial ones. The optimal value for the ration being established at 1-1-2.
- The obtained glasses were characterized from their capacity for immobilization of chromium, manganese and iron ions point of view.
- The hydrolytic stability of the studied glasses was measured. All of the glasses belong to HGB1 stability class, the best one according to ISO 719-1985. A quasilinear dependence of the hydrolytic stability upon the amount of R_2O, brought by borax and the glass waste, was established.
- The chemical stability of the glass samples was established by measuring the dissolution rate after 28 days in mediums having different pH. The low values recorded confirm the very good stability conferred by the glass matrix. The glasses present a high chemical stability towards the acidic and neutral environments, the recorded losses being between 0,011-0,022 μg/h. All the studied samples are more sensitive to the alkaline medium, the corresponding dissolution rates ranged from 0,153-0,195 μg/h. due to the absence of the passivation layer.
- No manganese losses were recorded, regardless the time and aggressive solution used.
- The chromium ions leached in the three aggressive environments after 7, 14 and 28 days according to the American Extraction Procedure Toxicity Test were very low, ranging from 0-0,0121% of the total chromium brought by the exhausted reactive mixtures.
- The amount of iron ions leached from all the investigated glasses regardless the environment's pH and the considered time is very low, between 0-0,0026% of the total iron brought by the exhausted reactive mixtures.
- The higher amount of losses of both chromium and iron ions are generated by the alkaline environment that leach SiO_2 and B_2O_3, both network former oxides, generating a continuous aggressive attack on the vitreous matrix..
- The obtained results confirm the viability of the suggested solution for immobilizing chromium contained in the exhausted reactive mixtures together with common glass wasted in order to obtain glasses having very high chemical stability with multiple economic advantages.

3.2 Immobilization of the retained chromium from exhausted reactive mixtures containing Fe(0) in ceramic matrices

The aim of this study was to immobilize the chromium ions retained in the exhausted reactive mixtures in ceramic matrices together with Bojidar kaolin.

3.2.1 Experimental procedure

The oxidic composition of the Bojidar kaolin is presented in table 9 (Goleanu et al., 2004).

Table 9. Oxidic composition of the Bojidar kaolin [%]

Oxide	Bojidar kaolin
SiO_2	49,29
Na_2O	0,14
K_2O	0,87
CaO	0,56
MgO	0,44
Al_2O_3	35,18
Fe_2O_3	0,78
TiO_2	0,43
P.C.	12,31

Considering that the 4 exhausted reactive mixtures have the same composition and granulometry, differing by the way the manganese oxide was coated, the sample used for the following investigations was the one from the column 2, having the highest amount of retained chromium (124 mg).

Three initial ratios exhausted reactive mixture:kaolin were tested: 2:1, 1:1 and 1:2. The homogenization process was realized by wet grinding using a Pulverisette laboratory mill. The mixture was dried at 120^{o}C for 6h and then pressed into cylinders having the diameter and height around 35 mm using an uniaxial Greisinger Electronics M.P 150 D press using 6 tf.

The thermal treatment was conducted at 800, 900 and 1000^{o}C for 90 minutes using a Nabertherm HTC08/16 electric furnace.

The ceramic samples obtained using the exhausted reactive mixture:kaolin ratio 2:1 present after the thermal treatment a large number of cracks extended in the whole volume being thereby unfit for further investigations.

3.2.2 Preliminary investigations

The following determinations were focused on the optimization of the initial compositions in order to achieve the highest chromium and iron immobilization in the ceramic matrices.

3.2.2.1 The apparent porosity of the ceramic samples

The apparent porosity represents the contribution of the open pores to the total porosity of a porous material being calculated as follows:

$$P_{ap} = \frac{\rho_a \cdot a}{\rho_0} \ [\%] \quad (9)$$

where: - ρ_a represents the apparent density of the material [g/cm^3];

- ρ_0 represents the density of the working fluid [g/cm^3];
- *a* represents the absorption capacity of the studied material.

The apparent porosity of the obtained ceramics was measured using the liquid saturation method under vacuum with water as working liquid.

The values of the apparent porosity for the samples obtained at 800, 900 and 1000^{o}C are presented in the table 10 for the two exhausted reactive mixture:kaolin ratios 1:1 and 1:2.

Table 10. The apparent porosity (P_{ap}) of the obtained ceramic samples

P_{ap}[%]					
exhausted reactive mixture:kaolin 1:1			**exhausted reactive mixture:kaolin 1:2**		
800˚C	**900 ˚C**	**1000 ˚C**	**800˚C**	**900 ˚C**	**1000 ˚C**

30.11	26.50	19.75	33.25	30.50	24.25

3.2.2.2 The chromium ions immobilization in the initial ceramic samples

The high values of the apparent porosity presented in table 10 lead to the assumption that theses samples may have high chromium losses due to the large sample's specific surface exposed to the chemical aggression. Therefore the chromium dissolution from the initial samples was studied according to the American Extraction Procedure Toxicity Test, the obtained results are presented in the table 11.

Table 11. Chromium ions leached from the initial ceramics for the exhausted reactive mixture:kaolin ratio 1:1 and 1:2 respectively

Ratio	**Chromium leached [%]**								
	800˚C			**900 ˚C**			**1000 ˚C**		
	pH=5.5	**pH=7**	**pH=8.5**	**pH=5.5**	**pH=7**	**pH=8.5**	**pH=5.5**	**pH=7**	**pH=8.5**
1.1	8.2111	8.4340	11.2225	7.6625	7.9930	10.0115	5.2115	5.0095	7.1255
1.2	8.6215	8.6468	11.9545	8.4185	8.4898	11.2155	6.9575	6.9445	9.8475

The chromium ions losses for both considered ratios are high regardless the thermal treatment temperature, ranged from 5,01 – 11,95%.

Based on the previous data, the forwards investigations will focus on the reduction of the apparent porosity of the ceramic samples, knowing that the high specific surface associated to this porosity is the main cause for the low immobilization of chromium. Therefore common glass wastes such as window panes and cathode ray tubes were used together with the exhausted reactive mixture and the kaolin. The thermal treatment was conducted at 1000^{o}C, considered optimal based on the previous data, in order to assure a fluid melt generated from the glass precursors, able to fill the pores in the ceramic matrix.

3.2.3 Synthesis of ceramic samples containing glass wastes

The two glass wastes used as precursors: window panes and cathode ray tubes (CRT) were grind and dried as described in the chapter 3.1.1. Together with the exhausted reactive mixtures and the kaolin they were homogenized using a Pulverisette laboratory mill. Three different ratios mixture:kaolin:glass were used: 1:1:1, 1:2:1 and 1:1:2. The ceramic samples obtained using the last ratio after the thermal treatment presented important dimensional and shape deviations due to the high amount of liquid phase generated by the large glass quantity and therefore they are excluded from the further investigations. The compositions of the studied ceramics are summarized in the table 12.

Table 12. Ceramic samples composition (weight ratio)

Sample	**Bojidar Kaolin**	**Exhausted reactive mixture**	**Glass waste**	
			Window pane	**CRT**
1.1G-C	1	1	1	-
1.2G-C	1	2	1	-
1.1E-C	1	1	-	1
1.2E-C	1	2	-	1

3.2.4 Properties of the ceramic samples containing glass

Considering the objective of this study – to immobilize the exhausted reactive mixtures containing chromium – the investigated properties for the obtained ceramics were the apparent porosity, the phase composition and the chemical resistance towards chemical aggression.

3.2.4.1 The apparent porosity of the obtained ceramics

The importance of this property that affect the chemical resistance of the ceramic samples was discussed in the chapter 3.2.2.2. The values of the apparent porosity for the samples obtained at 1000^{o}C, measured using the liquid saturation method under vacuum with water as working liquid are presented in the table 13.

Table 13. Apparent porosity (P_{ap}) of the studied ceramics

Sample	P_{ap}[%]
1.1G-C	3.55
1.2G-C	3.80
1.1E-C	2.35
1.2E-C	2.65

The apparent porosity of all the synthesized ceramics are lower compared to those obtained without the glass wastes precursors, ranging from 2,35 - 3,80%. This behavior is due to the liquid phase resulted by melting the glass wastes at 1000^{o}C. The CRT glass, more fluid than the window panes glass wastes due to it's composition generates a lower porosity for the corresponding ceramic samples as it can be observed on the SEM images obtained using a Quanta FEG 250 microscope, presented in the figure 26 for two representative ceramic samples.

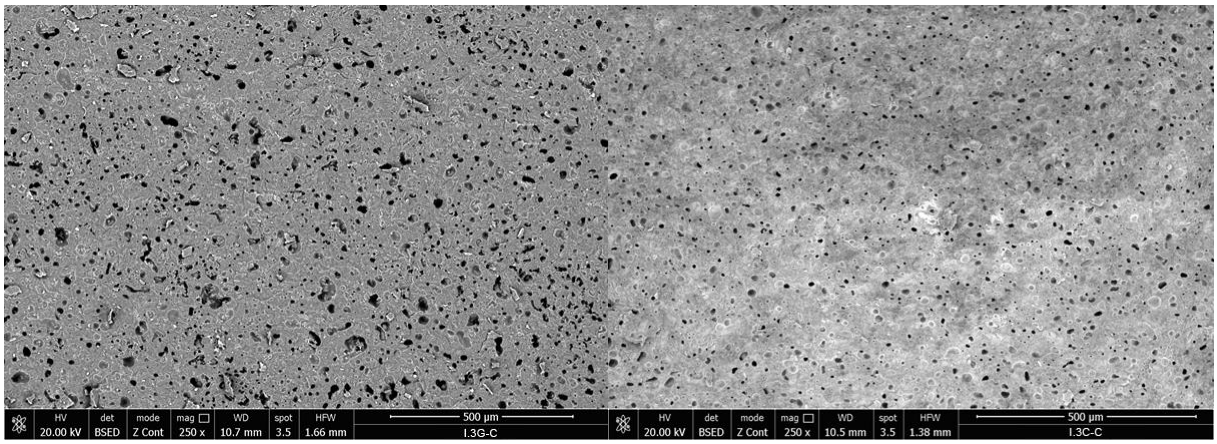

a. b.

Fig.26. The microporous structure of the samples: a - 1.1G-C; b - I.1E-C.

Both samples present a microporous structure characterized by a relatively uniform distribution of the pores in the ceramic matrix with a narrow dimensional spectra, all pores having micrometric dimensions.

3.2.4.2 Phase composition of the studied ceramics

The nature of studied samples was investigated using a Rigaku Ultima 4 diffractometer. The obtained results for the samples 1.1G-C and 1.1E-C containing window panes and CRT glass wastes respectively are presented in the figure 27

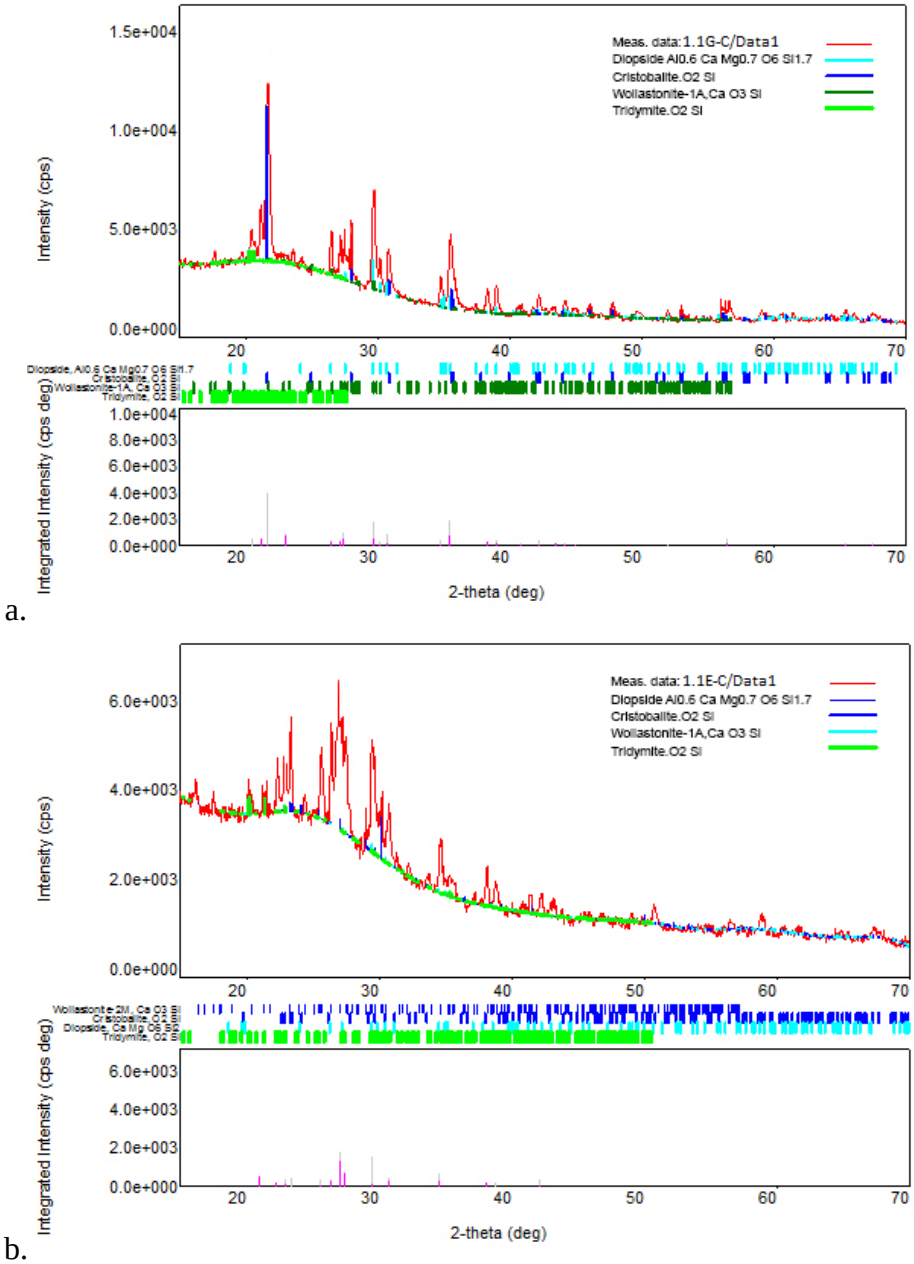

Fig. 27. Diffraction spectra of the samples: a - 1.1G-C; b - 1.1E-C.

The main crystalline phases in both samples, having different glass waste precursors, are wollastonite, tridymite, diopside and cristobalite. The presence of tridymite can be accounted for the sand that comes with the kaolin while the cristobalite is generated by the recrystallization process of the amorphous SiO_2 as it is presented by the reactions 10.

$$Al_2O_2 \cdot 2SiO_2 \cdot 2H_2O \xrightarrow{450-700℃} Al_2O_2 \cdot 2SiO_2 + 2H_2O_{(g)}$$
$$2(Al_2O_2 \cdot 2SiO_2) \xrightarrow{925-1050℃} 2Al_2O_2 \cdot 3SiO_2 + SiO_{2\ (amorphous)} \qquad (10)$$

$$3(Al_2O_2 \cdot 3SiO_2) \xrightarrow{\geq 1050^{\circ}C} 2(3Al_2O_2 \cdot 2SiO_2) + 5SiO_2$$

$$SiO_{2(amorphous)} \xrightarrow{\geq 1200^{\circ}C} SiO_{2(crystobalite)}$$

The diopside is generated by the reaction of the amorphous SiO_2 resulted from the thermal decomposition of the kaolinite with CaO and MgO from the glass melt.

3.2.4.3. Chemical stability of the ceramic samples

The values for the chemical stability, measured by the samples' dissolution rate as it was presented in the chapter 3.1.2.3 are summarized in the table 14

Table 14. Dissolution rate values [μg/h] for the studied ceramic samples

Sample	pH		
	pH=5.5	pH=7	pH=8.5
1.1G-C	0.166	0.164	0.589
1.2G-C	0.142	0.177	0.715
1.1E-C	0.148	0.143	0.552
1.2E-C	0.139	0.141	0.448

The increasing of the apparent porosity leads to a rise of the dissolution rate values and a reduction of the chemical stability for all the investigated ceramic samples due to the higher specific surface exposed to the chemical aggression.

3.2.4.4. Chromium and iron ions immobilization in the ceramic matrices

The chromium and iron immobilization capacity of the studied ceramics were measured according to the American Extraction Procedure Toxicity Test as it was presented in the chapter 3.1.2.4.

The lixiviation values for chromium, calculated as percentage of chromium leached from the total chromium introduced by the exhausted reactive mixtures are presented in the table 15 and illustrated by the figure 28.

Table 15. Chromium ions losses from the investigated samples

Sample	Chromium ions leached [%]								
	7 days			14 days			28 days		
	pH=5.5	pH=7	pH=8.5	pH=5.5	pH=7	pH=8.5	pH=5.5	pH=7	pH=8.5
1.1G-C	0.0000	0.0000	0.0482	0.0181	0.0205	0.0748	0.0225	0.0228	0.1710
1.2G-C	0.0000	0.0000	0.0425	0.0135	0.0132	0.0715	0.0216	0.0220	0.1697
1.1E-C	0.0000	0.0000	0.0345	0.0165	0.0126	0.0682	0.0196	0.0211	0.1314
1.2E-C	0.0000	0.0000	0.0335	0.0120	0.0119	0.0655	0.0182	0.0208	0.1184

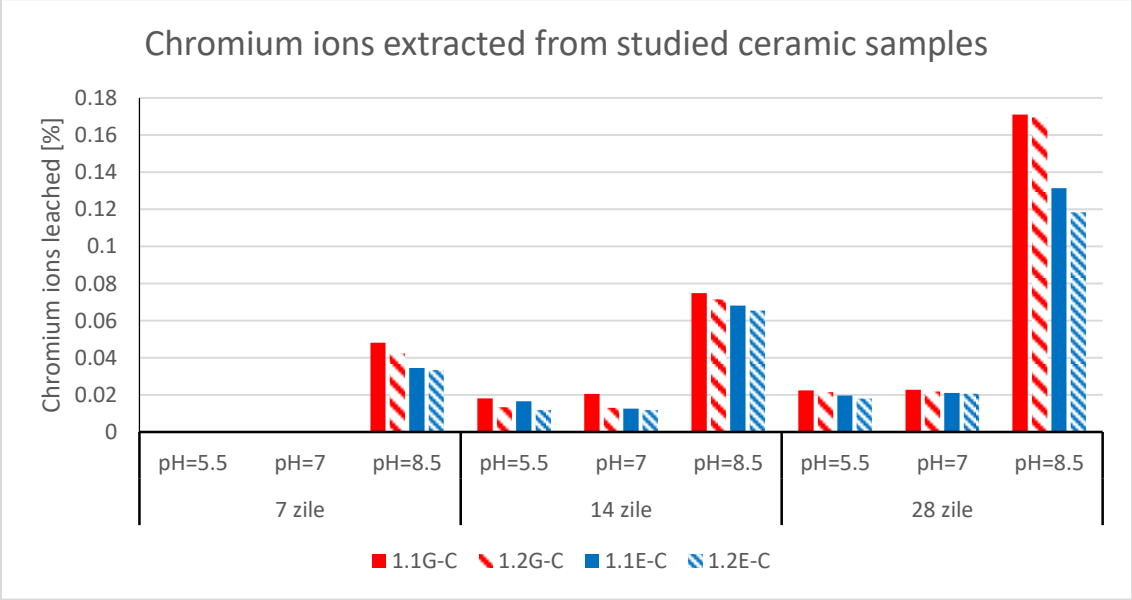

Fig. 28 Cromium ions losses from the ceramic containing exhausted reactive mixtures.

The chromium ions lixiviation values from all the investigated ceramic samples regardless the environment's pH and the considered time are very low, ranging between 0-0,1710% of the total chromium brought by the exhausted reactive mixtures.

The ceramics obtained based on the exhausted reactive mixtures leads to samples having no discernable losses of chromium after 7 days, for acidic and neutral aggressive attacks. All the ceramic materials show low chromium losses in the alkaline medium, which increase by increasing the amount of chromium brought by the exhausted reactive mixture. The samples' apparent porosity play a key role in the chromium immobilization by increasing the specific surface exposed to the chemical attack. They were recorded low chromium losses for all samples after 14 and 28 days in the three used aggressive environments.

All the samples containing CRT glass wastes as precursors shows lower chromium losses due to lower porosity of the ceramics caused by the higher fluidity of these glass melt compared to the one generated by the windows panes wastes.

The described behavior for the chromium losses in all the ceramic samples suggests that the chromium ions are located in the glass phase, more sensible to the alkaline aggression comparing to the ceramic phases.

The lixiviation values for iron ions, calculated as percentage of iron leached from the total iron introduced by the exhausted reactive mixtures are presented in the table 16 and illustrated by the figure 29.

Table 16. Iron ions losses from the investigated samples

Sample	**Iron ions leached [%]**								
	7 days			**14 days**			**28 days**		
	pH=5.5	**pH=7**	**pH=8.5**	**pH=5.5**	**pH=7**	**pH=8.5**	**pH=5.5**	**pH=7**	**pH=8.5**
1.1G-C	0	0	0.0000	0.0205	0.0224	0.0671	0.0528	0.0538	0.1210
1.2G-C	0	0	0.0125	0.0285	0.0317	0.0725	0.0521	0.0602	0.1295
1.1E-C	0.0145	0.0148	0.0745	0.0472	0.0468	0.1282	0.0908	0.0911	0.1485
1.2E-C	0.0115	0.0107	0.0825	0.0495	0.0515	0.1443	0.0985	0.1020	0.1544

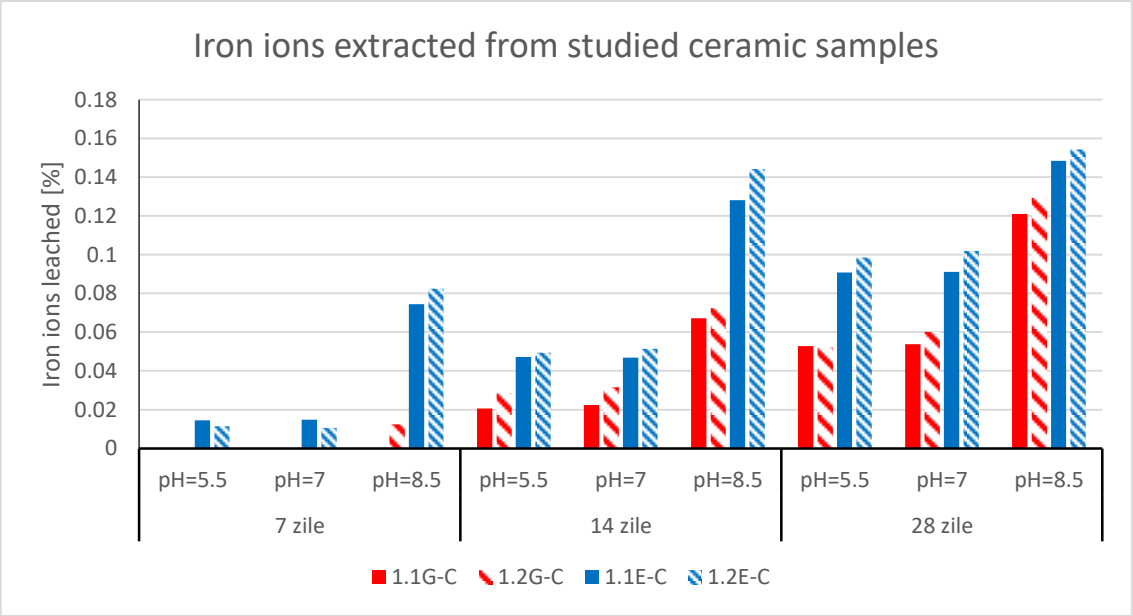

Fig. 29 Iron ions losses from the ceramic containing exhausted reactive mixtures.

The iron ions losses from all the investigated ceramic samples regardless the environment's pH and the considered time are very low, ranging between 0-0,1544% of the total iron brought by the exhausted reactive mixtures. The samples containing window pane wastes generates a complete immobilization of iron ions after 7 days towards the acidic and neutral aggression.

The described behavior for the iron losses in all the ceramic samples suggests that the iron ions are located prevalently in the ceramic matrix, and therefore being more sensible at the acidic and neutral aggression.

3.2.5 Conclusions

- The aim of this study was to immobilize the chromium and iron ions from the exhausted reactive mixtures in ceramic matrices together with Bojidar kaolin.
- Three different weight ratios exhausted reactive mixture-kaolin were tested: 2:1, 1:1 and 1:2. First set of samples generates after the heat treatment fragile and fractured ceramics, unfit for further investigations. The last two groups of samples had high apparent porosities, ranged between 19,75-33,25% that lead to important chromium losses, up to 11,95%. Those lixiviation values are too high to validate the proposed method as an alternative for chromium immobilization.
- The next experiments were focused on the porosity reduction in the ceramic samples, knowing that this is responsible for the chromium losses. Therefore windows panes and cathode ray tubes glass wastes were used together with the exhausted reactive mixtures and the kaolin. At the optimal heat treatment temperature, considered based on the previous tests to be 1000^{o}C, the two glass wastes generate liquid phase by melting, that is able to fill the open pores in the ceramic matrix and therefore to reduce the chromium losses.
- The apparent porosity for the ceramics containing glass wastes range between 2,35 - 3,80%, ten times lower than those based only on exhausted reactive mixture and kaolin, reflecting therefore the positive effect of using the glass wastes.

- The main crystalline phases the studied ceramics having different glass waste precursors, are wollastonite, tridymite, diopside and cristobalite.
- The chemical stability of the glass samples was established by measuring the dissolution rate after 28 days in mediums having different pH. The low values recorded confirm the very good stability conferred by the glass matrix. All the ceramic samples have higher chemical stability towards acidic and neutral aggression measured by dissolution rates of 0,139-0,177 μg/h than towards alkaline aggression where the mass losses range between 0,448-0,715 μg/h. That behavior support the conclusion that the glass phase is mainly affected by the chemical aggression compared to the more stable ceramic phases.
- The chromium ions leached in the three aggressive environments after 7, 14 and 28 days according to the American Extraction Procedure Toxicity Test were low, ranging between 0-0,1710% of the total chromium brought by the exhausted reactive mixtures.
- The behavior for the chromium losses in all the ceramic samples suggests that the chromium ions are located in the glass phase, more sensible to the alkaline aggression comparing to the ceramic phases.
- The amount of iron ions leached from all the investigated ceramic samples is very low, ranging between 0-0,1544% of the total iron brought by the exhausted reactive mixtures.
- The behavior for the iron losses in all the ceramic samples suggests that the iron ions are located prevalently in the ceramic matrix, and therefore are more sensible at the acidic and neutral aggression.
- The obtained results confirm the viability of the suggested solution for immobilizing chromium contained in the exhausted reactive mixtures together with common glass wasted and kaolin as ceramics having very high chemical stability with multiple economic advantages.

Objective 4. Dissemination of the obtained results

Activities: Analysis and interpretation of experimental data. Writing of scientific articles. Patent application.

The experimental data was analyzed, interpreted and disseminated, as following:

M. Gheju, I. Balcu, A. Enache, A. Flueras, A kinetic approach on hexavalent chromium removal with metallic iron, Journal of Environmental Management, 203, 2017, 937-941.

M. Gheju, I. Balcu, Assisted green remediation of chromium pollution, Journal of Environmental Management, 203, 2017, 920-924.

C. Vancea, M. Gheju, G. Moșoarcă, Inertization in vitreous matrix of exhausted reactive mixtures resulted from the removal of Cr(VI) with Fe^0 in continuous-flow system, Romanian Journal of Materials. Manuscript under review.

M. Gheju, I. Balcu, Mitigation of Cr(VI) aqueous pollution by reuse of iron-contaminated water treatment residues, ChemEngineering. Accepted manuscript.

M. Gheju, I. Balcu, Cheap metallic iron source for hexavalent chromium removal, The 4th International Conference on Energy and Environment Research, ICEER 2017, 17-20 July 2017, Porto, Portugal. Manuscript accepted for publication in Energy Procedia.

M. Gheju, Treatment of waters with metallic iron. WORKSHOP: "World water day", 22 March, 2017, Timișoara.

M. Gheju, Decontamination of hexavalent chromium-polluted waters: significance of metallic iron technology, in N. Anjum, S. Gill, N. Tuteja (eds.), Enhancing Cleanup of Environmental Pollutants. Volume 2 Non Biological Approaches. Springer International Publishing, 2017, pp. 209-254. ISBN 978-3-319-55422-8.

M. Gheju, I. Balcu, G. Mosoarca, C. Vancea, Synergic composition for treatment of waters polluted with hexavalent chromium. OSIM patent application No. A/00260/2017.

Objective 5. Project self-evaluation
Activities: Analysis of the achievement degree of the 2017 stage objectives

The degree of achievement of objectives for the 2017 stage was analyzed. It was concluded that all the proposed objectives were fully achieved, so there was no need to make any corrective action.

References

APHA, AWWA, WEF, 1995. Standard methods for the examination of water and wastewater, 19th edition. United Book Press, Inc., Baltimore.

Chaudhry S.A., Khan T.A., Ali I., Adsorptive removal of Pb(II) and Zn(II) from water onto manganese oxide-coated sand: isotherm, thermodynamic and kinetic studies, Egypt. J. Basic Appl. Sci., 2016, 3(3), 287-300.

Flury B., Eggenberger U., Mader U., First results of operating and monitoring an innovative design of a permeable reactive barrier for the remediaton of chromate contaminated groundwater, J. Appl. Geochem., 24, 2009, 687-697.

Gheju M., Iovi A., Kinetics of hexavalent chromium reduction by scrap iron, J. Hazard. Mater., B135 (1-3), 2006, 66-73.

Kapteijin F., van Langeveld A.D., Moulijn J.A., Andreini A., Vuurman M.A., Turek A.M., Jehng J.M., Wachs I.E., Alumina-supported manganese oxide catalyst. I Characterization: effect of precursor and loading, J. Catal. 1994, 150, 94-104.

Landrot G., Ginder-Vogel, Sparks D.L., Kinetics of chromium(III) oxidation by manganese(IV) oxides using quick Scanning X-ray Absorption Fine Structure Spectroscopy (Q-XAFS), Environ. Sci. Technol., 2010, 44, 143-149.

Ma Z., Zhu L., Xing S., Wu Y., Gao Y., Facile synthesis of Mn–Co oxide with a hierarchical porous structure for heavy metal removal, Mater. Let., 108, 2013, 261-263.

Maliyekkal S.M., Philip L., Pradeep T., As(III) removal from drinking water using manganese oxide-coated-alumina: Performance evaluation and mechanistic details of surface binding, Chem. Eng. J., 2009, 153, 101-107.

Manning B.A., Fendorf S.E., Bostick B., Suarez D.L., Asenic(III) oxidation and arsenic(V) adsorption reactions on synthetic birnessite, Environ. Sci. Technol., 2002, 36, 976-981.

Taffarel S.R, Rubio J., Removal of Mn^{2+} from aqueous solution by manganese oxide coated zeolite, Miner. Eng., 23, 2010, 1131-1138.
Tilak A.S., Ojewole S., Williford C.W., Fox G.A., Sobecki T.M., Larson S.L., Formation of manganese oxide coatings onto sand for adsorption of trace metals from groundwater, J. Environ. Qual., 2013, 42, 1743-1751.
Wekesa M., Uddin M.J., Sobhi H.F., An insight into Mn (II) chemistry: a study of reaction kinetics under alkaline conditions, Int. J. Chem. Res. 2(4), 2011.
Wilkin R.T., Su C., Ford R.G., Paul C.J., Chromium-removal processes during groundwater remediation by a zerovalent iron permeable reactive barrier, Environ. Sci. Technol., 39(12), 2005, 4599-4605.
Goleanu A., Lazău I., Apetri C., Lazău R.I., Corelatii între caracteristicile fizico-mineralogice şi proprietătile tehnologice ale unor caolinuri utilizate în industria portelanului, Revista Română de Materiale, 34 (3), 2004, 163.
ISO 719-1985, Glass - Hydrolytic resistance of glass grains at 98 degrees C - Method of test and classification.
Lazău I., Vancea C., New vitreous Matrix for the Chromium Wastes immobilization, Cent. Eur. J. Chem., 12(7), 2014, 763-768.